

Clinical, molecular, and cellular immunologic findings in patients with *SP110*-associated veno-occlusive disease with immunodeficiency syndrome

Simon T. Cliffe, BSc(Hons),^{a*} Donald B. Bloch, MD, PhD,^{b*} Santi Suryani, BSc(Hons), PhD,^c Erik-Jan Kamsteeg, PhD,^d Danielle T. Avery, BAppSci,^e Umaimainthan Palendira, BSc(Hons), PhD,^c Joseph A. Church, MD,^e Brynn K. Wainstein, MBBS, FRACP,^f Antonino Trizzino, MD,^g Gérard Lefranc, PhD,^h Carlo Akatcharian, MD,ⁱ André Megarbané, MD, PhD,^j Christian Gilissen, PhD,^d Despina Moshous, MD,^k Janine Reichenbach, MD,^l Siraj Misbah, MD,^m Uli Salzer, PhD,ⁿ Mario Abinun, FRCP,^o Peck Y. Ong, MD,^e Polina Stepensky, MD,^p Ezia Ruga, MD,^q John B. Ziegler, MD, FRACP,^f Melanie Wong, MBBS, PhD, FRACP,^r Stuart G. Tangye, BSc(Hons), PhD,^c Robert Lindeman, MBBS, PhD, FRACP,^a Michael F. Buckley, MBChB, PhD, FRCPA, FRCPATH,^a and Tony Roscioli, MBBS, PhD, FRACP^{a,s} Sydney, Australia, Boston, Mass, Nijmegen, The Netherlands, Los Angeles, Calif, Palermo and Padua, Italy, Montpellier and Paris, France, Beirut, Lebanon, Zurich, Switzerland, Oxford and Newcastle, United Kingdom, Freiburg, Germany, and Jerusalem, Israel

Background: Mutations in the *SP110* gene result in infantile onset of the autosomal recessive primary immunodeficiency disease veno-occlusive disease with immunodeficiency syndrome (VODI), which is characterized by hypogammaglobulinemia, T-cell dysfunction, and a high frequency of hepatic veno-occlusive disease.

Objectives: We sought to further characterize the clinical features, B-lineage cellular immunologic findings, and molecular pathogenesis of this disorder in 9 patients with new diagnoses, including 4 novel mutations from families of Italian, Hispanic, and Arabic ethnic origin.

Methods: Methods used include clinical review; Sanger DNA sequencing of the *SP110* gene; determination of transfected mutant protein function by using immunofluorescent studies in Hep-2 cells; quantitation of B-cell subsets by means of flow

cytometry; assessments of B-cell function after stimulation with CD40 ligand, IL-21, or both; and differential gene expression array studies of EBV-transformed B cells.

Results: We confirm the major diagnostic criteria and the clinical utility of *SP110* mutation testing for the diagnosis of VODI. Analysis of 4 new alleles confirms that VODI is caused by reduced functional *SP110* protein levels. Detailed B-cell immunophenotyping demonstrated that *Sp110* deficiency compromises the ability of human B cells to respond to T cell-dependent stimuli and differentiate into immunoglobulin-secreting cells *in vitro*. Expression microarray studies have identified pathways involved in B-lymphocyte differentiation and macrophage function.

Conclusion: These studies show that a range of mutations in *SP110* that cause decreased *SP110* protein levels and impaired

From ^athe Department of Haematology and Genetics, Prince of Wales Hospital, Sydney; ^bthe Centre for Immunology and Inflammatory Diseases, Massachusetts General Hospital, Boston and Harvard Medical School, Boston; ^cthe Immunology Program, Garvan Institute of Medical Research and St Vincent's Clinical School, University of New South Wales, Sydney; ^dthe Department of Human Genetics, Radboud University Nijmegen Medical Centre, Nijmegen; ^ethe Division of Clinical Immunology and Allergy, Childrens Hospital Los Angeles; ^fthe Department of Immunology & Infectious Diseases, Sydney Children's Hospital; ^gPediatric Hematology Oncology, Ospedale dei Bambini "G. Di Cristina," ARNAS Civico, Palermo; ^hthe Institute of Human Genetics, CNRS, UPR 1142, and Université Montpellier 2, Montpellier; ⁱthe Department of Pediatrics, Hospital Hôtel-Dieu de France, Saint Joseph University, Beirut; ^jthe Medical Genetics Unit, Faculty of Medicine, Saint Joseph University, Beirut; ^kFaculté de Médecine René Descartes, Université Paris Descartes, Site Necker, IFR94, Paris, and Assistance Publique-Hôpitaux de Paris, Hôpital Necker-Enfants Malades, Unité d'Immunologie et d'Hématologie Pédiatriques, Paris; ^lthe Division of Immunology/Haematology/BMT and the Children's Research Centre, University Children's Hospital Zurich, and the Zurich Centre for Integrative Human Physiology (ZIHP), University of Zurich; ^mthe Department of Clinical Immunology, Oxford Centre for Clinical Immunology, John Radcliffe Hospital, Oxford; ⁿthe Centre of Chronic Immunodeficiency (CCI), University Medical Center Freiburg and University of Freiburg; ^othe Department of Paediatric Immunology, Newcastle General Hospital; ^pPediatric Hematology-Oncology and BMT, Hadassah University Hospital, Jerusalem; ^qthe Department of Pediatrics, University of Padova, Padua; ^rthe Department of Allergy, Immunology and Infectious Diseases, the Children's Hospital, Westmead, Sydney; and ^sthe School of Women and Children's Health, Sydney Children's Hospital and the University of New South Wales, Sydney.

*These authors contributed equally to this work.

Infrastructure support was provided by the Department of Haematology and Genetics, South Eastern Area Laboratory Services, Sydney, and the Department of Human Genetics, Radboud University, Nijmegen Medical Centre. D.B.B. is supported by a grant from the Massachusetts General Hospital. C.A. and A.M. were supported in part by the Research Council of the Saint Joseph University, Beirut. D.M. was supported by the Robert A Good/Jeffrey Modell Fellowship in Transplantation and Immunodeficiency. J.R. was supported by the Gebert Ruff Stiftung, Program Rare Diseases-New Approaches, grant no. GRS-046/10. S.G.T. is an NHMRC Senior Research Fellow with research funding provided by NHMRC Program Grant no. 427620. M.F.B. is the recipient of a Marie Curie Fellowship (PIIF-GA-2008-221048) from the EU Science Directorate. T.R. is supported by an Australian NHMRC postdoctoral research fellowship.

Disclosure of potential conflict of interest: D. Moshous has received research support from the Jeffrey Modell Foundation. J. Reichenbach has received research support from the Chronic Granulomatous Disorder Research Trust and Gebert Ruff Stiftung. M. F. Buckley has received research support from the European Union Directorate of Science. The rest of the authors declare they have no relevant conflicts of interest. Received for publication August 9, 2011; revised January 19, 2012; accepted for publication February 21, 2012.

Available online May 21, 2012.

Corresponding author: Michael F. Buckley, MBChB, PhD, FRCPA, Department of Haematology and Genetics, Prince of Wales Hospital, Barker Street, Randwick 2031, Sydney, Australia. E-mail: michael.buckley@sesiahs.health.nsw.gov.au.

0091-6749/\$36.00

© 2012 American Academy of Allergy, Asthma & Immunology

doi:10.1016/j.jaci.2012.02.054

late B-cell differentiation cause VODI and that the condition is not restricted to the Lebanese population. (J Allergy Clin Immunol 2012;130:735-42.)

Key words: *Veno-occlusive disease with immunodeficiency, hypogammaglobulinemia, SP110, B-cell development*

Familial veno-occlusive disease with immunodeficiency syndrome (VODI; Online Mendelian Inheritance in Man [OMIM] 235550) is an autosomal recessive immunodeficiency syndrome with specific clinical features.¹ The key features of VODI include (1) severe hypogammaglobulinemia, (2) clinical evidence of T-cell dysfunction, (3) hepatomegaly with evidence of hepatic failure or histologically proved hepatic veno-occlusive disease (hVOD) in the proband or a first-degree relative that is unexplained by iatrogenic factors, (4) a pattern of disease transmission consistent with autosomal recessive inheritance, and (5) onset before the age of 12 months.

VODI is caused by mutations in the *SP110* gene (see Fig E1 in this article's Online Repository at www.jacionline.org).¹ The role of *SP110* in patients with VODI was identified through homozygosity mapping in consanguineous families of Lebanese origin who were unable to form germinal centers, resulting in absent plasma cells and hypogammaglobulinemia.¹ *SP110* is a single-copy gene in humans; however, in all inbred strains of laboratory mice, it is part of a rearranged and amplified genomic region containing approximately 60 to 2000 copies of *Sp110* and 20 adjacent genes.²⁻⁴ An important consequence of this genomic rearrangement is that it has not yet been feasible to produce a genetic knockout of *Sp110* by means of gene targeting in mice. Currently, the only readily available means to understand the pathogenesis of VODI is through the analysis of *SP110*-deficient cells from patients with VODI.

VODI was described initially in patients of Lebanese descent, and the perception that VODI is restricted to that population means that VODI might not be considered in patients with severe immunodeficiencies of other ethnic backgrounds. Here we extend studies into VODI through the analysis of B-cell function in a larger cohort of patients with VODI, describing the phenotypes in 9 further patients, 4 of whom have novel mutations in *SP110* (2 Italian, 1 Arabic, and 1 Hispanic). We present additional data on the cellular immunologic defect in patients with VODI, demonstrating an absence of CD10⁻CD27⁺ B memory cells and intrinsic B-cell response to T-cell stimulation. Gene expression studies in patients' B cells showed altered expression of several immunologic genes, suggesting additional studies into the biology of VODI.

METHODS

Subjects

Patients with a clinical or immunologic presentation consistent with VODI were tested for mutations in *SP110*. Mutations were identified in patients 1, 2, 4, 5, and 10 to 16 at South East Area Laboratory Services, Sydney, Australia. Molecular studies in patient 3 were carried out at Hadassah University Hospital, Jerusalem, Israel. Patients 6 to 9 were studied at the Hôtel-Dieu de France Hospital and the Unit of Medical Genetics, Saint Joseph University, Beirut, Lebanon, in collaboration with the Laboratoire d'Immunogénétique Moléculaire, Institut de Génétique Humaine, Montpellier, France.

Immunologic methods

The frequencies of transitional (CD20⁺CD10⁺CD27⁻), naive (CD20⁺CD10⁻CD27⁻), and memory (CD20⁺CD10⁻CD27⁺) B cells were

Abbreviations used

BMT:	Bone marrow transplantation
CD40L:	CD40 ligand
CMV:	Cytomegalovirus
DAVID:	Database for Annotation, Visualization and Integrated Discovery
hVOD:	Hepatic veno-occlusive disease
IVIG:	Intravenous immunoglobulin
SAM:	Statistical Analysis of Microarrays
VODI:	Veno-occlusive disease with immunodeficiency syndrome

determined in the peripheral blood of healthy donors and patients with *SP110* mutations after incubation with mAbs against CD20, CD10, and CD27 and flow cytometry.⁵⁻⁷ The proportion of CD21^{lo} and CD21^{hi} transitional B cells, which correspond respectively to early and late populations of transitional B cells, were determined as previously described.⁸ The expression of immunoglobulin isotypes on naive and memory B cells was determined as previously described.⁹ B-cell function in patients with VODI with *SP110* mutations was analyzed by using several approaches.

First, total B cells were isolated from PBMCs collected from 3 patients with VODI and 5 control subjects by means of negative selection with DYNAL beads (DynaL Biotech, Oslo, Norway) achieving greater than 95% B-cell purity. These were then cultured *in vitro* (approximately 10 × 10³/200 μL) with recombinant CD40 ligand (CD40L) alone or together with IL-21 (50 ng/mL; PeproTech, Rocky Hill, NJ).

Second, naive B cells were sort-purified from patients (n = 3) and control subjects (n = 3) and then cultured as above. Secretion of IgM, IgG, and IgA was determined after 10 to 12 days of culture.¹⁰

A detailed description of the molecular methods is provided in the Methods section in this article's Online Repository at www.jacionline.org.

RESULTS

Clinical descriptions

The clinical features of 9 newly ascertained children with VODI were compared with the findings in 7 historical cases (Table I). The age at presentation ranged from 2 to 11 months. The presenting features included cytomegalovirus (CMV)-related hepatitis (patient 1), respiratory distress (patient 2), fever and respiratory symptoms (patient 4), and failure to thrive, respiratory distress, and diarrhea (patient 5), with neonatal testing before disease onset in 1 case (patient 3). Pathogen isolation included disseminated CMV infection (hepatic, oropharyngeal, and vulval in patient 1), rotavirus-related gastroenteritis, and respiratory *Pneumocystis jiroveci* (patients 4 and 5). Among the entire group of 16 patients, clinical hepatosplenomegaly was detected in 12 patients at presentation. Results of hepatic biopsy in patient 1 were consistent with hVOD, and PCR of the hepatic biopsy material was positive for CMV.

Idiopathic cerebrospinal leukodystrophy was present in 3 of 16 patients (patients 5, 6, and 10), suggesting that this complication should be sought in patients with VODI. The leukodystrophy in patient 6 occurred after CMV-related gastroenteritis and resulted in lower limb paralysis that is resolving. Patients 5 and 10 had idiopathic central nervous system leukodystrophy. Unique patient features included inappropriate antidiuretic hormone secretion (patient 5) and pulmonary fibrosis (patient 2).

The mortality rate for VODI was previously reported as 100% in the first year of life. In contrast, there have been only 3 deaths among the 8 newly ascertained patients older than 1 year, representing a markedly improved prognosis with early

TABLE I. Clinical features of patients with *SP110* mutations and their VODI-affected relatives

Patient	<i>SP110</i> mutation	Age of diagnosis and general/hepatic presenting features	Other clinical and histologic findings	Alive/deceased
Patients reported in this study				
Patient 1, Italian	c.319_325dup exon 4	Age 11 mo: hepatosplenomegaly, disseminated CMV infection, rotavirus-related gastroenteritis, vulvar abscesses, hVOD	Recovering from hVOD, well	Alive
Patient 2, Italian	c.667+1dup exon 5	Age 3 mo: hepatosplenomegaly, failure to thrive, respiratory distress/lung fibrosis, diarrhea	Hepatic biopsy consistent with sinusoidal dilatation and moderate central vein and perivenular subsinusoidal fibrosis; stable with improvement	Alive
Patient 3, Palestinian Arabic	c.373del exon 4	Age 3 mo: diagnosis of VODI confirmed with cascade testing before illness onset; no hepatomegaly or liver function abnormalities	Stable and well	Alive age 2 mo
Patient 4, Hispanic	c.78_79delinsAT exon 2	Age 5 mo: Hepatomegaly, fever, respiratory distress, pancytopenia	Recovered from hVOD, stable and well	Alive
Patient 5, Lebanese	c.642del exon 5	Age 3 mo: respiratory distress	SIADH, idiopathic cerebrosplinal leukodystrophy	Alive
Patient 6, Lebanese	c.642del exon 5	Age 3 mo: chronic cough, diarrhea hepatosplenomegaly noted at age 8 y, hVOD from age 12 y	Raised PT from age 2 y, idiopathic left frontal lobe white matter calcified cyst at 7 y, delayed puberty to 18.5 y, blunted mammary development, irregular menses, epilepsy, CMV-related colitis, postdiarrheal encephalomyelitis with lower limb paralysis, cerebrosplinal leukodystrophy, esophageal candidiasis, duodenal lymphocytic infiltrate at 8 y, treated regular IMIG 3 mo to 9 y and IVIG subsequently	Alive age 21 y
Patient 7, Lebanese	c.642del presumed	Age 2 mo: chronic diarrhea, failure to thrive, middle ear and respiratory infections, hepatosplenomegaly, thrombocytopenia	Microcephaly, Hepatic biopsy consistent with hVOD	Deceased, 11 mo diarrhea leading to septic shock
Patient 8, Lebanese	c.642del presumed	Age 5 mo: upper respiratory tract illness, age 8 mo chronic diarrhea, hepatomegaly, thrombocytopenia	Hepatic biopsy consistent with hVOD	Deceased, 3.5 y, diarrhea leading to septic shock
Patient 9, Lebanese	c.642del presumed	Age 2 mo: ascites, hepatomegaly, anemia, thrombocytopenia	Hepatic biopsy consistent with hVOD	Deceased, 2.5 mo otitis, diarrhea, pneumonia
Previously reported patients*				
Patient 10	c.642del exon 5	Age 5 mo: immunodeficiency, thrombocytopenia, hVOD	Left hemiparesis secondary to leukodystrophy, recurrent hVOD with GVHD after HSCT	Deceased
Patient 11 ¹	c.642del exon 5	Age 4 mo: hepatosplenomegaly, ascites, hVOD, thrombocytopenia, mucocutaneous candidiasis	Chronic liver disease, portal hypertension posthepatic transplantation	Deceased
Patient 12	c.642del exon 5	Age 7 mo: immunodeficiency	Chronic lung disease secondary to recurrent aspiration	Deceased (age 19 y)
Patient 13	c.642del exon 5	Age 6 mo: hepatosplenomegaly, ascites, hVOD	Well	Alive
Patient 14	c.642del exon 5	Age 3 mo: hepatosplenomegaly, ascites, hVOD	Hemophagocytic syndrome after hepatic transplantation	Deceased
Patient 15	c.40del exon 2	Age 3 mo: immunodeficiency, thrombocytopenia, hepatosplenomegaly without definite evidence of hVOD	Enteroviral and <i>P jiroveci</i> infection	Deceased
Patient 16	c.642del exon 5	Age 3 mo: hepatosplenomegaly, ascites, hVOD	Pulmonary hemorrhage, multiorgan failure	Deceased

Modified from Roscioli et al.¹ Although patients 6 to 12 are not known to be related, they are believed to share a recent common ancestor. Patients 10 to 13 were included in the initial homozygosity mapping analysis. IgA and IgM serum concentrations increased to the lower limit of normal while receiving IVIG.

GVHD, Graft-versus-host disease; HSCT, hematopoietic stem cell transplantation; IMIG, intramuscular immunoglobulin; PT, prothrombin time; SIADH, syndrome of inappropriate secretion of antidiuretic hormone.

*Patients 10 to 15 are, respectively, AII.1, BII.1, CII.1, CII.2, DII.1, and E from Roscioli et al¹ plus an additional unreported patient (patient 16).

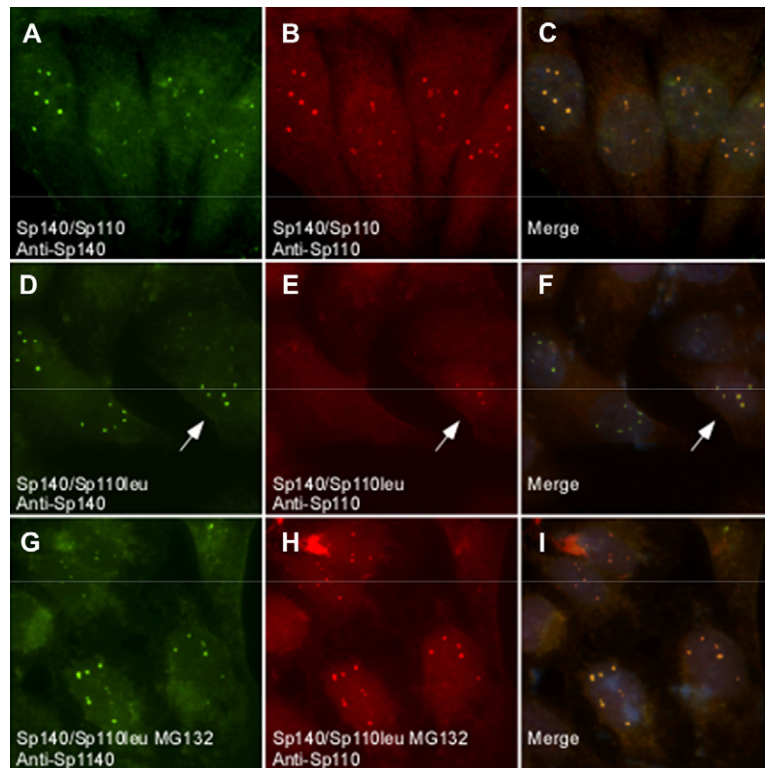


FIG 1. Coexpression of SP140 (A, D, and G, green), wild-type SP110 (B, red), and mutant SP110^{I27L} (SP110leu; E and H, red). The merged fluorescence images in Fig 1, A and B, D and E, and G and H, are shown in panels C, F, and I, respectively. DAPI staining in Fig 1, C, F, and I, indicates the location of nuclei.

recognition and treatment with intravenous immunoglobulin (IVIG) and *P jiroveci* prophylaxis. Patient 10 died after hVOD recurrence after bone marrow transplantation (BMT) at age 6 years. Two patients died after complications following hepatic transplantation: patient 11 with chronic hepatic disease and portal hypertension and patient 14 with hemophagocytic syndrome. The 5 patients who have survived are receiving *P jiroveci* pneumonia prophylaxis with cotrimoxazole and IVIG. Patients 1 and 4 remain stable on this treatment, whereas patients 2 and 5 have shown slow improvement. Patient 6, having survived into adulthood, has been treated with monthly IVIG and 300 mg of pentamidine di-isethionate at intervals of 6 to 8 weeks. Patient 3 comes from a family in which 2 of 3 children with VODI who were BMT recipients were cured and have been long-term survivors.

In an effort to further understand the specificity of the VODI phenotype for *SP110* mutations, this gene was sequenced in additional patients with atypical but overlapping features of VODI. No *SP110* mutations were detected in 5 additional patients with overlapping phenotypes referred for *SP110* mutation screening. The clinical features of this group are provided in the Results section in this article's Online Repository at www.jacionline.org.

SP110 mutation detection and validation

Four novel homozygous *SP110* mutations were detected in the new VODI cohort, bringing the total number of known disease alleles to 6 (Table I). The novel allele in patient 1 is a homozygous 7-bp tandem duplication in exon 4, c.319_325dup, which is predicted to cause a frame-shift mutation, p.(Ser109Trpfs), with the introduction of a premature stop codon 5 codons 3' of the

mutation. Quantitative PCR of SP110 mRNA extracted from a lymphoblastoid cell line from this patient showed a reduction in SP110B mRNA expression to levels of $38\% \pm 2.1\%$ and a reduction in SP110C expression to levels of $28\% \pm 4.4\%$ compared with those seen in control subjects, which is consistent with nonsense-mediated decay.

The novel allele in patient 2 causes the duplication of the final base of exon 5, c.667+1dup. The levels of SP110B and SP110C mRNA were reduced to $36\% \pm 2.7\%$ and $66 \pm 1.9\%$, respectively, compared with those of control subjects, which is consistent with this mutation acting as a frameshift mutation, with the introduction of a premature stop 4 codons 3' of the mutation resulting in nonsense-mediated mRNA decay.

The mutation in patient 3 is a single base pair deletion in exon 4, c.373del, which is predicted to result in a frameshift mutation, p.(Thr125Leufs), with premature protein truncation occurring 3 codons 3' of the mutation. Patient mRNA was not available for further analysis.

Patient 4 has the first missense mutation in VODI, a deletion/insertion mutation, c.78_79delinsAT, involving the third base of codon 26 and the first base of codon 27, p.(Ile27Leu). The predicted substitution has a Grantham distance of 5 but is predicted to be damaging by using PolyPhen2 (score = 0.949) because it is located within the highly conserved N-terminal SP100 domain.¹¹⁻¹³ To test whether the mutant protein could still be incorporated into nuclear bodies, plasmids encoding SP110^{wt} or SP110^{I27L} were cotransfected with SP140^{wt} into SP110- and SP140-nonexpressing Hep-2 cells.¹³ Coexpression of SP140^{wt} (Fig 1, A, D, and G, green signal) and SP110^{wt} (Fig 1, B, red signal) resulted in colocalization of both proteins in nuclear bodies.

TABLE II. Immunologic findings in 6 patients with VODI

	Patient no.*					
	1	2	3	4	5	6
Age	11 mo	7 mo	1 wk	9 mo	7 mo	21 y
Mutation in <i>SP110</i> †	c.319_325dup	c.667+1dup	c.373del	c.78_79delinsAT	c.642del	c.642del
IgG	139‡	55‡	NN	83‡	353§	781§
IgA	15‡	1‡	NN	<7‡	8‡,§	<22‡,§
IgM	24‡	6‡	NN	<7‡	4‡,§	<17.7‡,§
Total lymphocyte count (× 10 ⁹ /L)	2.33‡	4.8	5.0	—	1.83	0.28-0.7‡,
CD3 (× 10 ⁹ /L)	1.8‡	2.6	4.0	1.3‡	0.58‡	0.20-0.46‡,
CD4 (× 10 ⁹ /L)	1.1‡	3.6	3.0	0.74‡	0.46‡	0.11-0.23‡,
CD8 (× 10 ⁹ /L)	0.68	1.1	0.9	0.58	0.13‡	0.03-0.12‡,
CD19 (× 10 ⁹ /L)	0.21‡	2.0	0.15‡	1.1	1.13	0.05-0.15‡,
NK cells CD16, CD56 (× 10 ⁹ /L)	NA	0.1‡	0.85	NA	0.05‡	0.013-0.07‡,
HLA-DR (× 10 ⁹ /L)	0.26	NA	NA	NA	0.04‡ (0.17-0.39)	NA

NA, No result available; NN, neonatal.

*Patient numbering follows that used in Table I.

†Reference sequence NM_080425.2.

‡Low value for age.¹⁵

§Receiving IVIG therapy: the immunoglobulin levels in patient 6 were measured immediately before immunoglobulin infusion and represent the mean of 7 observations.

||Range of the values for 6 observations made between the ages of 15 and 21 years.

When SP140^{wt} and SP110^{I27L} were coexpressed, SP140 was detected in nuclear bodies (Fig 1, D), but only very low levels of SP110^{I27L} were detected (Fig 1, E). In rare cells SP110^{I27L} was detected by using indirect immunofluorescence and was observed to colocalize with SP140 (Fig 1, D, E, and F, white arrow). These results show that although the overall level of SP110^{I27L} was markedly reduced in transfected cells, the residual SP110^{I27L} was capable of being imported into nuclear bodies.

SP140 and SP110^{I27L} were expressed in Hep-2 cells and cultured in the presence of the proteasome inhibitor MG132 to explore whether SP110^{I27L} protein instability could account for these findings.¹⁴ After 4 hours of exposure to MG123, SP110^{I27L} was easily detected in transfected cells (Fig 1, H, red signal), which is consistent with the SP110^{I27L} protein being subject to enhanced proteasome degradation. These data suggest that marked reductions in SP110 protein levels are the major pathogenic mechanism underlying VODI in this patient.

Immune phenotyping in patients with VODI

Comparisons were made for B- and T-cell subsets between patients 1 and 6 (Table II).¹⁵ In contrast with a previous report, the majority of patients with VODI had reduced circulating T-cell numbers, B-cell numbers, or both for their age.¹⁶ Subsets of human B cells can be resolved by the differential expression of CD10, CD21, and CD27 and other cell-surface antigens into subclasses of transitional, naive, and memory B cells (Table III). The proportion of B cells that were memory cells was significantly reduced in patients with VODI compared with published reference ranges and age-matched control subjects (2.1% ± 0.8% vs 28.7% ± 6.2%, *P* = .0085). Analysis of the contracted population of memory B cells in 2 patients with VODI demonstrated an absence of immunoglobulin isotype-switched cells (not shown). Thus mutations in *SP110* not only impair the generation of memory B cells but also impair the ability of B cells to undergo immunoglobulin class-switching. The distribution of subsets of transitional B cells was also altered, with a significant increase in the proportions of the less mature CD21^{lo} transitional B cells (52.1% ± 3.6% vs 32.0% ± 6.9%, *P* < .05) and a corresponding decrease in the

TABLE III. Immunophenotyping in patients with *SP110* mutations and control subjects

Age (y)	CD20 ⁺ B cells (%)			Transitional B cells (%)		
	Transitional (%)	Naive (%)	Memory (%)	CD21 ^{lo}	CD21 ^{hi}	
Cases (patients with VODI)						
1	~5	47.1	42.4	4.89	44.9	55.1
1*	5	17.2	74.7	4.06	60.4	39.6
4	3	44.9	51.4	1.09	55.5	44.5
5	4.5	35	63.5	0.45	ND	ND
13	13	29.8	68.7	0.97	47.4	52.6
13*	16	16.4	81.6	1.3	ND	ND
Mean		31.7‡	63.7	2.1‡	52.05†	47.95†
SD		13.2	14.6	1.9	7.2	7.2
SE		5.3	6.0	0.76	3.6	3.6
Control subjects						
1	2.3	4.35	8.96	58.2	13.7	86.3
2	14	8.75	60.4	27.3	31.4	68.6
3	1.6	31.4	42.3	22.5	47.0	53.0
4	2.1	12.2	57.2	28.7	35.9	64.2
5		13.6	68.2	16.1	ND	ND
6		9.2	68.9	19.1	ND	ND
Mean		13.3	51	28.7	32.0	68.03
SD		9.5	22.7	15.2	13.8	13.8
SE		3.9	9.3	6.2	6.9	6.9

ND, Not determined.

Significance testing: †*P* < .05 and ‡*P* < .01.

*Samples collected from patients at different times.

more mature population of CD21^{hi} transitional cells (48.9% ± 3.6% vs 68.0% ± 6.9%, *P* < .05) in patients with VODI (Table III). Together, these findings suggest a specific role for SP110 in the differentiation of naive B cells into memory B cells or the survival of these effector B cells.

To extend the observations of a defect in memory B-cell generation in patients with VODI, we examined patients' B cells for their ability to undergo *in vitro* differentiation into immunoglobulin-secreting cells. Comparison of total B cells from healthy donors and patients with VODI revealed an

TABLE IV. Immunoglobulin secretion in response to CD40L ± IL-21

	Immunoglobulin secretion (ng/mL)							
	Control subjects		Patient 1		Patient 4		Patient 13	
Total B cells	CD40L	+ IL-21	CD40L	+IL-21	CD40L	+ IL-21	CD40L	+ IL-21
IgM	742 ± 384	32,315 ± 8,433	3.9 ± 0.2	11,300 ± 786	16.5 ± 1.5	4,081 ± 462	42.5 ± 1.0	920 ± 54
IgG	22 ± 14	12,661 ± 6,660	0.6 ± 0.1	290 ± 7.1	0	135 ± 8	5.7 ± 4.7	30.8 ± 6.2
IgA	63 ± 26	17,700 ± 7,200	6.3 ± 0	221 ± 161	7.0 ± 0.2	56.1 ± 11.8	1.9 ± 0.3	9.2 ± 2.4

	Immunoglobulin secretion (ng/mL)							
	Control subjects		Patient 1		Patient 5		Patient 13	
Naive B cells	CD40L	+ IL-21	CD40L	+ IL-21	CD40L	+ IL-21	CD40L	+ IL-21
IgM	18.7 ± 9.8	4,087 ± 2,245	2.5 ± 0.2	541 ± 42	4.8 ± 2.7	4.8 ± 2.7	5.6 ± 0.5	222 ± 19
IgG	0	13.3 ± 8.4	0	1.7 ± 1.5	0	0	0	0.27 ± 0.04
IgA	0	105 ± 36	0	0	0	0	0	0

impairment of B cells from patients with VODI to produce IgM (6-fold reduced), IgG (>100-fold reduced), and IgA (>100-fold reduced) in response to stimulation with CD40L and IL-21 (Table IV). These differences did not simply reflect differences in the composition of the B-cell populations in control subjects and patients because analysis of flow-sorted naive B cells generated similar results, with naive B cells from patients with VODI producing 10-fold less IgM and being unable to produce IgA (3/3 patients) and IgG (2/3 patients) in response to CD40L/IL-21 (Table IV). The decreased ability of B cells from patients with VODI to secrete immunoglobulin after culture with CD40L/IL-21 was replicated in cultures with CD40L/CpG, in which secretion of IgM by naive B cells from patients with VODI was also approximately 10-fold compared with that seen in naive B cells of healthy subjects (experiment 1: control subjects, 2235 ± 295 ng/mL IgM; patient 13, 254 ± 7 ng/mL; experiment 2: control subjects, 1200 ± 90 ng/mL IgM; patient 1, 88 ± 16 ng/mL). These results were also independently confirmed in patient 2 by the lack of increased immunoglobulin production from PBMCs cultured with an anti-CD40 mAb and IL-10. In summary, *SP110* mutations compromise the intrinsic ability of B cells to respond to T cell-dependent stimuli and differentiate into immunoglobulin-secreting cells *in vitro*.

The compromised differentiation of naive B cells to immunoglobulin-secreting cells might well reflect a general defect in the activation and survival of B cells from patients with VODI, which would be consistent with the reduction in absolute numbers of lymphocytes in these patients. Naive B cells were isolated from the blood of patient 5, labeled with carboxyfluorescein succinimidyl ester, and then cultured with CD40L alone or together with IL-21 to investigate this further. After 5 days, cell proliferation was determined by assessing dilution of carboxyfluorescein succinimidyl ester. Although IL-21 strongly promoted the expansion of normal naive B cells, the effects of IL-21 on the proliferation of B cells from patients with VODI were markedly reduced (ie, only 65% of B cells from patients with VODI had entered division compared with >95% of normal naive B cells). Consistent with this reduced level of proliferation was a marked diminution in the frequency of naive B cells from patients with VODI that underwent isotype switching to acquire expression of IgG in response to CD40L/IL-21 stimulation (<0.5% B cells from patients with VODI vs 2.3% normal naive B cells), a differentiation event that is linked to cell division.¹⁵ It was also apparent from this analysis that a greatly reduced proportion of naive B cells from patients with VODI survived *in vitro*. Specifically, 33% and 61% of normal B cells were recovered

from cultures stimulated with CD40L and CD40L/IL-21, respectively; however, only 2.2% and 8.6% of B cells from patients with VODI were viable at the time of harvest. Thus B cells harboring mutations in *SP110* exhibit greatly diminished responses *in vitro* compared with their healthy counterparts; this in part results from reduced survival and subsequent proliferation rather than the gene mutation selectively abolishing the ability of naive B cells to undergo differentiation into immunoglobulin-secreting cells. The impaired survival and activation of B cells *in vitro* most likely explains the hypogammaglobulinemia that is typical of patients with VODI. This could also contribute to the memory B-cell deficiency in these patients.

Expression microarray analysis of EBV-transformed B-lymphoblastoid cells

The molecular pathogenesis of VODI is incompletely understood. Gene expression microarray studies were performed on EBV-transformed B cells from 4 patients with VODI who were homozygous for the mutation c.642del together with 5 control subjects. The Statistical Analysis of Microarrays (SAM) software identified 216 known protein-encoding genes that showed greater than 1.5-fold expression differences between patients with VODI and control subjects (see Fig E2 and Table E1 in this article's Online Repository at www.jacionline.org). Microarray results were validated by using a TaqMan Gene Expression Assay (AB Life Technologies, Carlsbad, Calif) based on the mean case/control expression differences among 14 selected genes ($r^2 = 0.88$). Notably, *CD27* and *SP110* showed approximately 3- to 5-fold mRNA downregulation, whereas *SP100* and *SP140* showed normal expression levels consistent with the known cause of VODI.

The 216 differentially expressed protein-coding genes were analyzed by using the Database for Annotation, Visualization and Integrated Discovery (DAVID) version 6.7 software to identify functional annotations with multiple gene expression differences.^{17,18} The most biologically relevant annotation cluster contained differentially expressed immune system genes involved in B- and T-cell activation/differentiation ($P = .0065$), the majority of which were also present in the Resource of Asian Primary Immunodeficiency Diseases (RAPID) database of known and candidate primary immunodeficiency genes.¹⁹ A systematic search of the RAPID database for differentially expressed genes identified 4 known genes (*ADA*, *CIITA*, *SP110*, and *TNFRSF13C*) and 14 candidate primary immune deficiency genes (*IRAK3*, *REL*, *PTK2*, *TNFSF4*, *STK17B*, *RUNX1*, *CD83*, *ANXA5*, *HOXB7*, *LY9*, *ZBTB32*, *CD27*, *SIT1*, and *HLA-C*), as well as 3 immunoregulatory

proteins (*AIM2*, *IL12A*, and *CD84*). Analysis of differentially regulated genes identified many with roles either in late B-cell differentiation or immunity to mycobacterial infections that are features of SP110 deficiency in human subjects and a murine model, respectively.

DISCUSSION

Until this point, the diagnosis of VODI has been confined to persons of Lebanese descent. The identification of 4 new alleles from Italian, Arabic, and Hispanic patients both broadens the mutation spectrum and indicates that the diagnosis of VODI should be considered in any child who presents with the combination of hypogammaglobulinemia and hepatic disease.

Overall, the clinical findings in the 9 newly identified patients validate the previously published clinical guidelines for a VODI diagnosis.¹ The majority of patients with *SP110* mutations presented before 6 months of age, except for a single patient (patient 1, c.319_325dup) who presented at 11 months of age. The immune phenotype was consistent between the 2 groups and characterized by hypogammaglobulinemia in all, reduced memory B cells with either a mild lymphopenia in the majority, or normal lymphocyte numbers. Virtually all patients had hepatic failure or hepatomegaly at the time of presentation. A significant improvement in the VODI recovery rate from 20% in the initial group to 100% in the recently identified group was identified. Similarly, a reduced mortality at a given age has been noted in the more recent cohort. BMT has been curative in 2 of 4 children with VODI. These findings suggest that earlier disease recognition and improved VODI management have resulted in reduced early mortality and that BMT, when carried out early before disease onset, might be successful.

A striking new finding is the presence of neurological abnormalities, notably cerebrosplinal leukodystrophy in 3 (20%) patients with VODI. Patient 5 had a leukodystrophy of unknown cause, and patient 6 developed this complication after CMV-related gastroenteritis. In patient 10 the initial diagnosis of Toxoplasmosis or a porencephalic cyst was revised to being more consistent with cerebrosplinal leukodystrophy. We speculate that the frequency of cerebrosplinal leukodystrophy might have been previously underestimated. Lung fibrosis of unknown cause was identified only in patient 2 (*SP110* c.667+1dupG).

The range of mutational events that have been described in patients with VODI has been significantly extended in this study to include 3 new frameshift mutations and 1 missense mutation. All reported mutations are homozygous, cluster within the first part of the gene (exons 2, 4, and 5) and predicted to affect all mRNA isoforms of *SP110*. The dinucleotide deletion/insertion mutation involves a highly conservative amino acid substitution that nevertheless produces profound effects on SP110 protein stability. Therefore the key pathogenic event in the development of VODI in all cases reported to date appears to be a lack of fully functional SP110 protein.

The B-cell immunodeficiency seen in patients with VODI is characterized by hypogammaglobulinemia, absence of memory B cells, lymph node germinal centers, and tissue plasma cells but is distinguished from other defects of late B cells, such as hyper-IgM syndrome and common variable immunodeficiency, by the involvement of CD4⁺ T memory cells. Here we have confirmed that patients with VODI have a severe deficiency of switched memory B cells. Such B-cell deficits might be due to either an

intrinsic inability of B cells to undergo isotype switching, as seen in patients with hyper-IgM syndrome caused by mutations in *CD40LG* or *AICDA*, or a T-cell defect of costimulation, as has been demonstrated for *ICOS* mutations in patients with common variable immunodeficiency and *SH2D1A* mutations in patients with X-linked lymphoproliferative syndrome. Naive B cells obtained from 3 patients with VODI secreted 20% of the normal levels of IgM and 1% of the normal levels of IgG and IgA in response to CD40L plus IL-21 costimulation, which is consistent with a block in B-cell differentiation between naive and “early” germinal center B cells and before the establishment of memory B cells.²⁰ Therefore the molecular pathogenesis of VODI most likely involves the disruption of a pathway affecting initial events underlying B-cell activation required for their entry into germinal centers and subsequent differentiation and survival as effector memory and plasma cells.

Expression microarray studies provide a well-validated mechanism to characterize the molecular changes underlying cellular phenotypes. This study demonstrated altered expression affecting several late B-cell differentiation pathways. One involved a 3-fold decrease in the expression of CD27. It is of interest that several other members of the TNF receptor superfamily were also shown to have altered expression patterns that might affect B-cell function.^{21,22} *TNFRSF13C/BAFFR* was found to be downregulated approximately 2-fold. Binding of B cell-activating factor of the TNF family to its receptor encoded by the *TNFRSF13C* gene delivers a powerful survival signal to B-cell receptor-positive B cells.²³ The identification of 2- to 2.8-fold decreased expression for 2 members of the SLAM family in cells from patients with VODI, *LY9 (SLAMF3/CD229)* and *CD84 (SLAMF5)*, is also consistent with the failure of production of memory B cells in patients with VODI because these molecules are expressed at increased levels on memory B cells compared with naive B cells.²⁴ In contrast, the gene encoding the T- and B-cell antigen CD83 demonstrated a 2.5-fold increase in its expression. Overexpression of CD83 has been associated with inhibition of late maturation of B cells.²⁵

SP110 deficiency leads to supersusceptibility to mycobacterial infection in the C3HeB/FeJ murine strain, but patients with VODI do not appear to be at increased risk of mycobacterial diseases. Gene expression differences between cells from patients with VODI and control cells, however, implicate SP110 deficiency in disturbances of IL-12/IFN- γ pathways, which play pivotal roles in the resistance to mycobacterial infection.²⁶ Expression of *IL12A* encoding the IL-12 p35 subunit was reduced 5.7-fold either as the direct consequence of lack of SP110 expression or possibly indirectly as a result of the 5- to 10-fold increased expression of *IRAK3*, both of which have been implicated in a reduction in the ability of macrophages to control mycobacterial infection.²⁷ The 5.5-fold increased expression of *REL*, a member of the nuclear factor κ B family of transcription factors, which is capable of inducing IL-12 expression, might result from feedback initiated by the reduction of IL-12. Annexin 5 also shows decreased expression in this dataset, possibly as a consequence of decreased signaling through the IFN- γ receptor as a result of decreased IFN- γ production.²⁸ Cells from patients with VODI have also been shown to have a 5.8-fold reduction in *AIM2* expression. *AIM2* is involved in sensing of intracellular pathogens through the binding of bacterial/viral DNA and subsequent triggering of the caspase-1-mediated proinflammatory cytokines, which ultimately leads to macrophage cell death.²⁹ The extensive disturbance

seen in mediators of mycobacterial infection control in the differential gene expression studies suggests that *SP110* deficiency influences pathways of mycobacterial resistance in both human subjects and mice but that the genomic alteration of the *Sp110* region either alone or in combination with other genetically linked events might contribute to the supersusceptibility phenotype of the C3HeB/FeJ murine strain.

In conclusion, the major findings in this report include confirmation of the major diagnostic criteria for VODI and the clinical utility of *SP110* mutation testing in non-Lebanese patients with hypogammaglobulinemia and hVOD. The discovery of 4 new disease alleles confirms that the major pathogenetic mechanism for this disorder involves reduction of functional protein levels either because of frameshift mutation with premature truncation or protein instability. Patients with VODI have a greatly reduced ability to produce IgM but are also unable to switch to IgG or IgA, resulting in a susceptibility to opportunistic infections. Patients with VODI are unable to form germinal centers, resulting in a reduced frequency of memory B cells and hypogammaglobulinemia. The VODI B-cell phenotype is reminiscent of the primary immunodeficiency disorders in which the formation of germinal center B cells is compromised. The T-cell immune profile in patients with VODI shows the absence of CD4⁺/CD45RO⁺/CD27⁻ memory T cells, which might contribute to T cell-dependent infection susceptibility, such as *P jiroveci*. Central memory and effector memory functions are therefore impaired in both cell lineages; however, it is unclear whether the susceptibility to *P jiroveci* is related to T- or B-cell impairment. Expression microarray studies have identified pathways involved in changes in mRNA levels of genes involved in B-lymphocyte differentiation and macrophage function. Taken together, these studies have provided insight into some of the molecular changes underlying the observed VODI phenotypes and represent a rich source of observations for further investigation.

C.A., A.M., and G.L. are particularly indebted to the Lebanese patient and her parents for their continued cooperation. They acknowledge warmly also all the members of the Unit of Medical Genetics, Pediatrics and Immunology Departments, Faculty of Medicine, Hospital Hôtel-Dieu de France, Saint Joseph University, Beirut, Lebanon, for their invaluable help.

Clinical implications: Infants with hypogammaglobulinemia and hVOD should be screened for mutations in the *SP110* gene, regardless of ethnic origin.

REFERENCES

- Roscioli T, Cliffe ST, Bloch DB, Bell CG, Mullan G, Taylor PJ, et al. Mutations in the gene encoding the PML nuclear body protein Sp110 are associated with immunodeficiency and hepatic veno-occlusive disease. *Nat Genet* 2006;38:620-2.
- Traut W, Rahn IM, Winking H, Kunze B, Weichenhan D. Evolution of a 6-200 Mb long-range repeat cluster in the genus *Mus*. *Chromosoma* 2001;110:247-52.
- Weichenhan D, Kunze B, Winking H, van Geel M, Osoegawa K, de Jong PJ, et al. Source and component genes of a 6-200 Mb gene cluster in the house mouse. *Mamm Genome* 2001;12:590-4.
- Agulnik S, Plass C, Traut W, Winking H. Evolution of a long-range repeat family in chromosome 1 of the genus *Mus*. *Mamm Genome* 1993;4:704-10.
- Avery DT, Ma CS, Bryant VL, Santner-Nanan B, Nanan R, Wong M, et al. STAT3 is required for IL-21-induced secretion of IgE from human naive B cells. *Blood* 2008;112:1784-93.
- Cuss AK, Avery DT, Cannons JL, Yu LJ, Nichols KE, Shaw PJ, et al. Expansion of functionally immature transitional B cells is associated with human immunodeficient states characterized by impaired humoral immunity. *J Immunol* 2006;176:1506-16.
- Wardemann H, Yurasov S, Schaefer A, Young JW, Meffre E, Nussenzweig MC. Predominant autoantibody production by early human B cell precursors. *Science* 2003;301:1374-7.
- Suryani S, Fulcher DA, Santner-Nanan B, Nanan R, Wong M, Shaw PJ, et al. Differential expression of CD21 identifies developmentally and functionally distinct subsets of human transitional B cells. *Blood* 2010;115:519-29.
- Ma CS, Hare NJ, Nichols KE, Dupre L, Andolfi G, Roncarolo MG, et al. Impaired humoral immunity in X-linked lymphoproliferative disease is associated with defective IL-10 production by CD4⁺ T cells. *J Clin Invest* 2005;115:1049-59.
- Ellyard JI, Avery DT, Phan TG, Hare NJ, Hodgkin PD, Tangye SG. Antigen-selected, immunoglobulin-secreting cells persist in human spleen and bone marrow. *Blood* 2004;103:3805-12.
- Nicewonger J, Suck G, Bloch D, Swaminathan S. Epstein-Barr virus (EBV) SM protein induces and recruits cellular Sp110b to stabilize mRNAs and enhance EBV lytic gene expression. *J Virol* 2004;78:9412-22.
- Seeler JS, Marchio A, Sitterlin D, Transy C, Dejean A. Interaction of SP100 with HPI proteins: a link between the promyelocytic leukemia-associated nuclear bodies and the chromatin compartment. *Proc Natl Acad Sci U S A* 1998;95:7316-21.
- Bloch DB, Nakajima A, Gulick T, Chiche JD, Orth D, de la Monte SM, et al. Sp110 localizes to the PML-Sp100 nuclear body and may function as a nuclear hormone receptor transcriptional coactivator. *Mol Cell Biol* 2000;20:6138-46.
- Dallaporta B, Pablo M, Maise C, Dugas E, Loeffler M, Zamzami N, et al. Proteasome activation as a critical event of thymocyte apoptosis. *Cell Death Differ* 2000;7:368-73.
- Shearer WT, Rosenblatt HM, Gelman RS, Oyomopito R, Plaeger S, Stiehm ER, et al. Lymphocyte subsets in healthy children from birth through 18 years of age: the Pediatric AIDS Clinical Trials Group P1009 study. *J Allergy Clin Immunol* 2003;112:973-80.
- Tangye SG, Avery DT, Hodgkin PD. A division-linked mechanism for the rapid generation of Ig-secreting cells from human memory B cells. *J Immunol* 2003;170:261-9.
- Dennis G Jr, Sherman BT, Hosack DA, Yang J, Gao W, Lane HC, et al. DAVID: Database for Annotation, Visualization, and Integrated Discovery. *Genome Biol* 2003;4:P3.
- Huang da W, Sherman BT, Lempicki RA. Systematic and integrative analysis of large gene lists using DAVID bioinformatics resources. *Nat Protoc* 2009;4:44-57.
- Keerthikumar S, Raju R, Kandasamy K, Hijikata A, Ramabadrans S, Balakrishnan L, et al. RAPID: Resource of Asian Primary Immunodeficiency Diseases. *Nucleic Acids Res* 2009;37:D863-7.
- Tangye SG, Good KL. Human IgM+CD27+ B cells: memory B cells or "memory" B cells? *J Immunol* 2007;179:13-9.
- Agematsu K, Nagumo H, Oguchi Y, Nakazawa T, Fukushima K, Yasui K, et al. Generation of plasma cells from peripheral blood memory B cells: synergistic effect of interleukin-10 and CD27/CD70 interaction. *Blood* 1998;91:173-80.
- Jacquot S, Kobata T, Iwata S, Morimoto C, Schlossman SF. CD154/CD40 and CD70/CD27 interactions have different and sequential functions in T cell-dependent B cell responses: enhancement of plasma cell differentiation by CD27 signaling. *J Immunol* 1997;159:2652-7.
- Mihalcik SA, Huddleston PM 3rd, Wu X, Jelinek DF. The structure of the TNFRSF13C promoter enables differential expression of BAFF-R during B cell ontogeny and terminal differentiation. *J Immunol* 2010;185:1045-54.
- Romero X, Benitez D, March S, Vilella R, Miralpeix M, Engel P. Differential expression of SAP and EAT-2-binding leukocyte cell-surface molecules CD84, CD150 (SLAMF6), CD229 (Ly9) and CD244 (2B4). *Tissue Antigens* 2004;64:132-44.
- Breloer M, Kretschmer B, Luthje K, Ehrlich S, Ritter U, Bickert T, et al. CD83 is a regulator of murine B cell function in vivo. *Eur J Immunol* 2007;37:634-48.
- Al-Muhsen S, Casanova JL. The genetic heterogeneity of Mendelian susceptibility to mycobacterial diseases. *J Allergy Clin Immunol* 2008;122:1043-53.
- Pathak SK, Basu S, Bhattacharyya A, Pathak S, Kundu M, Basu J. Mycobacterium tuberculosis lipaarabinomannan-mediated IRAK-M induction negatively regulates Toll-like receptor-dependent interleukin-12 p40 production in macrophages. *J Biol Chem* 2005;280:42794-800.
- Leon C, Nandan D, Lopez M, Moeenzakhanlou A, Reiner NE. Annexin V associates with the IFN-gamma receptor and regulates IFN-gamma signaling. *J Immunol* 2006;176:5934-42.
- Alnemri ES. Sensing cytoplasmic danger signals by the inflammasome. *J Clin Immunol* 2010;30:512-9.

METHODS

Mutation screening

Primers were designed that flanked each of the 19 exons included in the *SP110* mRNA isoform C (*SP110C*), as well as the alternately spliced exon 15a of *SP110B* (Fig E1). DNA was extracted from PBMCs by using standard protocols or from paraffin-embedded tissue samples by using a Qiagen DNeasy kit (Qiagen 69581, Holden, Germany). PCR was performed in a 20- μ L reaction volume containing 10 μ L of AmpliTaq Gold PCR Master Mix (Invitrogen, Carlsbad, Calif), 100 ng of genomic DNA, and 5 pmol of each of sense and antisense primers (primer sequences available on request). The thermocycling conditions used were initial denaturation at 95°C for 9 minutes followed by 32 amplification cycles (95°C for 30 seconds, 52°C for 10 seconds, 56°C for 20 seconds, 60°C for 20 seconds, and 72°C for 1 minute) and a final extension of 72°C for 7 minutes. Unincorporated primers were removed from PCR products by means of incubation at 37°C for 4 hours with 1 U of Shrimp Alkaline Phosphatase and 1U Exonuclease (GE Lifesciences, Fairfield, Conn) and cycle sequenced according to standard protocols for BigDye Terminator version 3.1 (AB Life Technologies). Sequencing products were analyzed on an ABI PRISM 3100xl Genetic Analyzer (AB Life Technologies).

Mutation validation

Cell culture. EBV-immortalized B-lymphoblastoid cell lines were generated by using standard procedures and grown as suspension cultures in RPMI 1640 (Gibco, Invitrogen, Carlsbad, Calif) supplemented with 25 mmol/L HEPES, 10% heat-inactivated FBS, 100 U/mL penicillin, 100 μ g/mL streptomycin, and 20 mmol/L L-glutamine and maintained in a humidified 5% CO₂ incubator at 37°C. Cell cultures were split 1:3 every 5 to 7 days and harvested for mRNA 48 hours after splitting.

RNA studies. Between 10⁷ and 10⁸ lymphoblastoid cells were washed in PBS, pH 7.4, and total RNA was extracted with Trizol reagents (15596026; Invitrogen, Carlsbad, Calif), and quantified by means of UV spectroscopy. cDNA was generated by using the Superscript III First Strand Synthesis System (18080051, Invitrogen) with 200 ng of starting RNA. Second-strand synthesis was performed with RealMasterMix+ROX (Eppendorf 2200700). TaqMan Gene Expression Assays (AB Life Technologies) were performed according to the manufacturers' instructions.

Quantitative PCR method. For the RNA experiments, TaqMan probes were selected that were specific to each *SP110* isoform (Hs894000_m1 [*SP110C*], Hs185406_m1 [*SP110B*], Hs897925_m1 [*SP110A*], and Hs893493_m1 [all *SP110*]), as well as to linked (Hs610654_m1 [*SP140*] and Hs162109_m1 [*SP100*]) and unlinked (Hs99999902_m1 [*RPLP0*]) control genes. For the microarray validation, the expression of several transcripts was quantitated to validate the results of the microarray *in toto*. Fourteen differentially expressed genes were selected, and their expression levels were measured by using TaqMan Gene Expression Assays (catalog no. 4331182), with 3 published housekeeping genes as endogenous controls (*GAPDH*, Hs99999905_m1; *RPLP0*, Hs99999902_m1; and *HPRT1*, Hs99999909_m1). The targets were as follows: *NDRG1*, Hs00608387_m1; *CYP11A1*, Hs00167984_m1; *ADAMTS6*, Hs01058097_m1; *RNF144B*, Hs00403456_m1; *EMILIN1*, Hs00170878_m1; *DPYD*, Hs00559279_m1; *RHOBTB3*, Hs00208554_m1; *STK17B*, Hs00177790_m1; *MUM1*, Hs00213970_m1; *BMPR2*, Hs00176148_m1; *COL4A3*, Hs00184277_m1; *LAG3*, Hs00158563_m1; *FGFR*, Hs100241111_m1; and *CXCL16*, Hs00222859_m1.

PCR mutagenesis

PCR mutagenesis was used to produce a cDNA that contained *SP110* mutations that mimicked the dinucleotide indel mutation in patient 4. The primers used were 5'-catgcaccagaagcttgggacgcctatgcattacacaagccatttc and its reverse complement, with the introduced mutations shown in italicized boldface font and the underlined base indicating an introduced silent *Hind*III restriction site. Fidelity of the entire *SP110* mutant cDNA was tested by means of DNA sequence analysis.

Cell culture, mammalian cell transfection, and immunohistochemistry

Hep-2 cells were obtained from American Type Culture Collection (Manassas, Va) and maintained in Dulbecco modified Eagle medium supplemented with 10% FBS, penicillin (200 U/mL), and streptomycin (200 mg/mL). Plasmids encoding SP140 and SP110^{wt} or SP110^{I27L} were transfected into Hep-2 cells by using the Effectene transfection system (Qiagen), as directed by the manufacturer. The preparation of rabbit anti-SP140 and rat anti-SP110 antisera was previously described.^{E1,E2} Species-specific and fluorescein- or rhodamine-conjugated secondary antisera were obtained from Jackson ImmunoResearch Laboratories (West Grove, Pa). Cells were fixed with 2% paraformaldehyde in PBS and permeabilized with 100% methanol for immunofluorescent staining. Cells were stained with primary and secondary antisera, as previously described.^{E3}

Microarray analyses

Cell lines from samples of 4 patients and 5 unrelated control subjects were cultured under the same tissue-culture conditions. The 4 patient cell lines were derived from 2 unrelated patients and a sib pair, all of whom were homozygous for the Lebanese founder mutation c.642del. Total RNA was extracted from EBV-transformed B cells by using a QIAGEN RNeasy Mini Kit (catalog no. 74106) and were processed at the Australian Genome Research Facility (www.agrf.org.au). Five hundred nanograms of total RNA was labeled with the Ambion Total Prep RNA amplification kit (catalog no. IL1791), and the quantity of labeled product was determined with an Agilent Bioanalyzer 2100 using the NanoChip protocol. Labeled RNA (1.5 μ g) in 30 μ L was hybridized to the Illumina WG-6 Human version 2.0 microarray platform (containing 48,701 probes targeting 42,648 transcripts; Illumina, San Diego, Calif) at 58°C for 16 hours on a rocking platform. After hybridization, nonspecifically bound RNA was removed according to the manufacturer's instructions, and the specifically bound Cy3-coupled RNA was detected with an Illumina BeadArray Reader. The BeadStudio software was used to convert the array signal for analysis.

Total RNA was isolated from cell cultures different than those used in the original microarray studies, converted to cDNA by using the Superscript III First-Strand Synthesis System (catalog no. 18080-051), and amplified by means of RT-PCR with 10 μ L of an Eppendorf RealMasterMix Probe ROX kit (Eppendorf AG, Hamburg, Germany), 1 μ L TaqMan Probe and Primer mix, and 8 μ L of cDNA. Quantitation was performed on a Corbett Research Rotorgene RG-3000 (denaturation at 95°C for 3 minutes and then 50 cycles of 95°C for 3 seconds and then 60°C for 30 seconds). Each sample underwent 6 replications for each probe and was normalized against the ROX signal. Relative expression ratios were calculated by using the 2^{- Δ ACT} method for each of the endogenous housekeeping genes and then averaged.

Analysis of microarray data

Measurable signals (Illumina Bead Studio detection $P < .05$) were detected for 15,144 (35.5%) probes in cells from at least 2 cases and 3 control subjects. Data were median normalized and analyzed by using the SAM software to identify gene expression differences. Unlogged data were formatted and manipulated with the SAM version 3.09 Addin for Microsoft Excel. The settings used included the 2-class unpaired response type, standard analysis type, and T-statistic without median centering of arrays. One thousand permutations of the data were performed with a minimum fold change threshold of 1.5 \times and a Δ value of 1.28, which yielded a predicted false discovery rate of 4.78%.^{E4} The list of differentially expressed genes was analyzed with the DAVID software (<http://niaid.abcc.ncifcrf.gov/>). DAVID recognized 216 (88.9%) of the 253 differentially expressed probes based on their Illumina probe ID as protein-encoding genes. DAVID functional annotations were analyzed under the high-classification stringency option with the background assigned as the Illumina WG-6_V2_0_R4_11223189_A gene set. Enrichment P values represent $1/\log_{10}$ of the probability that the functional annotations would be clustered by chance (cutoff $P = 1.30$, equal to a probability of 0.05).

RESULTS

Unconfirmed clinical cases with overlapping features

Five additional patients of Swiss, French/Antillean, Turkish, and English (n = 2) origins were referred for *SP110* mutation analysis given overlapping phenotypes with VODI. No *SP110* mutations were detected in this group. Two patients presented in the neonatal period. The Swiss patient presented with neonatal hepatopathy, failure to thrive, CMV infection, and *P jiroveci* pneumonia. The French/Antillean patient who presented on day 6 of life had fever, abdominal distension, and hepatomegaly/increased hepatic artery resistance, which are thought to be consistent with hVOD. An English girl presented at 2 months of age with severe failure to thrive, and investigations detected *P jiroveci* infection and adenoviral and group B hemolytic streptococcal sepsis. Hepatic ultrasonography detected gallbladder wall thickening and collateral venous circulation, and a postmortem examination detected sinusoidal congestion; however, hVOD was not present. The Turkish patient presented in childhood with severe recurrent respiratory tract infections with documented aspergilli, *Mycobacterium tuberculosis*, CMV, and Crohn disease. The only adult referral was a 35-year-old Englishman with probable common variable immunodeficiency but no infections to suggest a

significant cellular immune defect. Hepatic disease in this patient was investigated, and hVOD was identified.

The immune deficits in 4 of the 5 subjects included a predominantly T-cell lymphopenia with increased immunoglobulin levels (Swiss patient); predominance of T lymphocytes (98% CD3⁺), mostly CD4⁺ (84%), with no signs of activated T cells (French-Antillean patient); severe hypogammaglobulinemia, normal T-cell subsets, with normal proliferative responses (English patient); and agammaglobulinemia, absent B cells, normal T-cell numbers, and severely impaired cytokine production and a proliferation defect on mitogen stimulation (Turkish patient).

REFERENCES

- E1. Madani N, Millette R, Platt EJ, Marin M, Kozak SL, Bloch DB, et al. Implication of the lymphocyte-specific nuclear body protein Sp140 in an innate response to human immunodeficiency virus type 1. *J Virol* 2002;76:11133-8.
- E2. Bloch DB, Nakajima A, Gulick T, Chiche JD, Orth D de la Monte SM, et al. Sp110 localizes to the PML-Sp100 nuclear body and may function as a nuclear hormone receptor transcriptional activator. *Mol Cell Biol* 2000;20:6138-46.
- E3. Bloch DB, Yu JH, Yang WH, Graeme-Cook F, Lindor KD, Viswanathan A, et al. The cytoplasmic dot staining pattern is detected in a subgroup of patients with primary biliary cirrhosis. *J Rheumatol* 2005;32:477-83.
- E4. Tusher VG, Tibshirani R, Chu G. Significance analysis of microarrays applied to ionizing radiation response. *Proc Natl Acad Sci U S A* 2001;98:5116-21.

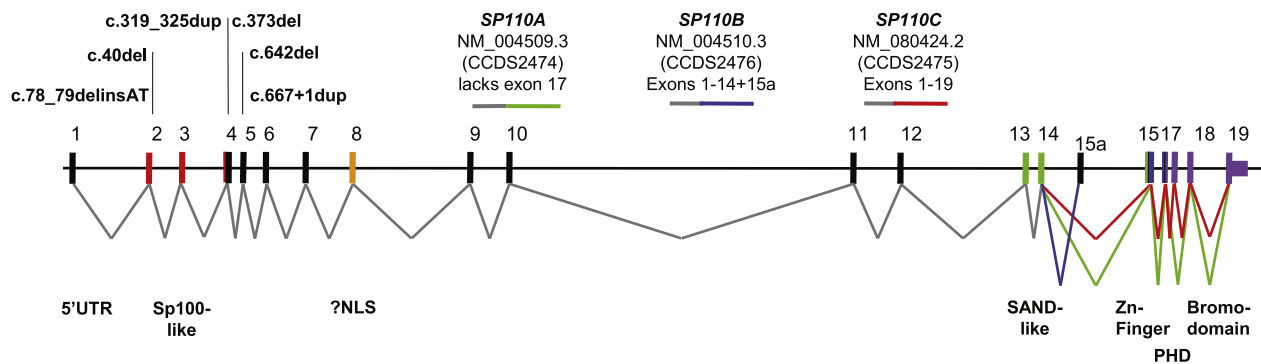


FIG E1. A model of the structure of *SP110* showing the positions of VODI-associated mutations, the alternate splicing pattern of the gene, and the *SP110* protein functional domains.

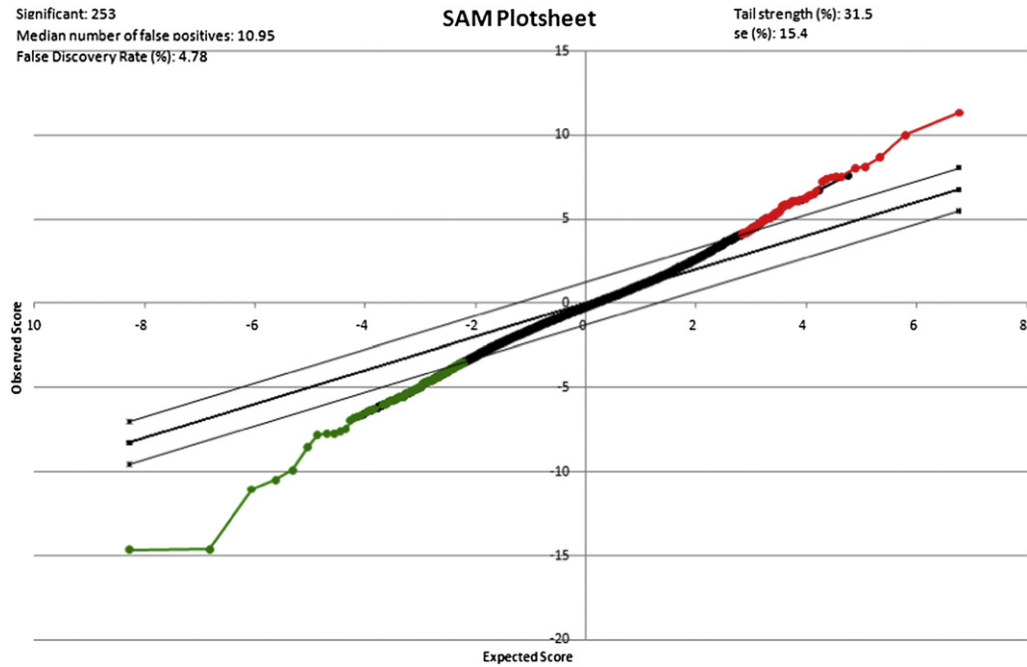


FIG E2. SAM plot of the actual intensity data with the observed SAM score plotted against the “expected” SAM score. The line representing observed = expected is in *black boldface*, whereas the *gray lines* indicate the significance threshold based on a Δ value of 1.28. The plot shows significantly different upregulated genes in *red (upper right)* and significantly different downregulated genes in *green (lower left)* listed in Table E1.

TABLE E1. List of 216 protein-encoding genes differentially expressed in cells from patients with VODI: Known and candidate primary immunodeficiency genes are highlighted

Gene symbol	Illumina ID	Fold change	t Test	Gene symbol	Illumina ID	Fold change	t Test	Gene symbol	Illumina ID	Fold change	t Test	Gene symbol	Illumina ID	Fold change	t Test
Upregulated protein-encoding genes				<i>BAZ2B</i>	ILMN_20026	1.90	6.02E-04	<i>EXOSC5</i>	ILMN_6934	-1.64	6.99E-03	<i>TSPAN9</i>	ILMN_30091	-2.22	1.16E-02
				<i>FYTTD1</i>	ILMN_5513	1.89	3.50E-03	<i>STT3A</i>	ILMN_17585	-1.65	4.25E-03	<i>AMFR</i>	ILMN_138270	-2.23	8.35E-03
<i>IRAK3</i>	ILMN_90041	9.61	3.62E-04	<i>FHOD1</i>	ILMN_14837	1.87	2.83E-02	<i>GARS</i>	ILMN_16659	-1.65	6.81E-04	<i>ASNS</i>	ILMN_14195	-2.24	2.71E-03
<i>MYH11</i>	ILMN_5070	8.24	1.37E-03	<i>ABCC10</i>	ILMN_4545	1.83	2.74E-03	<i>C18ORF19</i>	ILMN_17843	-1.66	2.36E-03	<i>NT5C3L</i>	ILMN_24101	-2.26	1.20E-04
<i>C4BPB</i>	ILMN_16247	7.71	1.60E-02	<i>MARCH2</i>	ILMN_137964	1.82	7.13E-03	<i>PLEKHA7</i>	ILMN_17656	-1.66	2.94E-03	<i>FAM119B</i>	ILMN_12426	-2.28	3.21E-03
<i>P2RX5</i>	ILMN_10544	7.40	1.70E-02	<i>FBXW7</i>	ILMN_18088	1.81	1.11E-02	<i>ARL5B</i>	ILMN_7087	-1.66	9.75E-03	<i>TMEM156</i>	ILMN_13771	-2.31	6.83E-03
<i>SPINT2</i>	ILMN_28039	5.56	1.20E-02	<i>TMSB15A</i>	ILMN_138276	1.79	1.31E-02	<i>GGH</i>	ILMN_9870	-1.66	5.40E-03	<i>DHRS2</i>	ILMN_25760	-2.32	7.06E-05
<i>IRAK3</i>	ILMN_25857	5.27	5.80E-03	<i>POPCD2</i>	ILMN_17743	1.77	2.84E-04	<i>ARMET</i>	ILMN_28822	-1.67	8.41E-03	<i>BCAS4</i>	ILMN_21706	-2.33	2.36E-04
<i>ROGDI</i>	ILMN_15661	4.98	5.21E-04	<i>EXOC2</i>	ILMN_3424	1.76	4.52E-04	<i>C19ORF44</i>	ILMN_21329	-1.67	3.48E-03	<i>SLC6A9</i>	ILMN_8399	-2.38	8.23E-04
<i>HMHB1</i>	ILMN_4838	4.69	1.40E-03	<i>SUSD1</i>	ILMN_29846	1.75	1.05E-03	<i>OPLAH</i>	ILMN_11581	-1.67	8.71E-03	<i>SLC43A1</i>	ILMN_20441	-2.49	3.32E-04
<i>ZEB2</i>	ILMN_14685	4.65	1.31E-03	<i>CUX1</i>	ILMN_8630	1.74	1.22E-02	<i>PDIA4</i>	ILMN_4575	-1.69	4.18E-04	<i>LRIG3</i>	ILMN_16293	-2.74	1.02E-02
<i>TRIB2</i>	ILMN_1571	4.51	1.35E-02	<i>ACP2</i>	ILMN_3044	1.74	4.60E-03	<i>SQSTM1</i>	ILMN_22135	-1.70	5.39E-03	<i>WBP5</i>	ILMN_3272	-2.78	1.04E-02
<i>VPS37B</i>	ILMN_18457	4.38	1.30E-02	<i>PHF23</i>	ILMN_20271	1.73	4.96E-03	<i>AARS</i>	ILMN_29917	-1.71	4.55E-03	<i>CD84/SLAMF5</i>	ILMN_16790	-2.81	2.26E-03
<i>C13ORF18</i>	ILMN_19053	4.34	2.16E-04	<i>SESN1</i>	ILMN_5404	1.73	2.63E-03	<i>GNPDA1</i>	ILMN_29056	-1.71	9.08E-03	<i>TCEA3</i>	ILMN_27218	-2.96	3.38E-03
<i>HIP1R</i>	ILMN_46681	3.90	2.48E-04	<i>GNA15</i>	ILMN_15421	1.72	5.62E-03	<i>CDT1</i>	ILMN_18895	-1.72	8.05E-03	<i>UPP1</i>	ILMN_21817	-3.01	1.37E-04
<i>C21ORF91</i>	ILMN_19108	3.88	1.45E-04	<i>TM7SF3</i>	ILMN_7797	1.69	2.92E-03	<i>C21ORF57</i>	ILMN_21121	-1.73	3.30E-02	<i>LRRC26</i>	ILMN_41107	-3.08	2.59E-03
<i>DPYD</i>	ILMN_19002	3.82	7.16E-03	<i>SUMF1</i>	ILMN_15497	1.67	1.36E-03	<i>CSorf45</i>	ILMN_15322	-1.73	8.49E-03	<i>SLC45A3</i>	ILMN_12972	-3.12	2.00E-03
<i>KCNMB4</i>	ILMN_2977	3.74	1.03E-02	<i>MKLI</i>	ILMN_25866	1.61	2.96E-03	<i>EMP3</i>	ILMN_7403	-1.75	1.08E-02	<i>MANEAL</i>	ILMN_11393	-3.14	5.09E-03
<i>CFP</i>	ILMN_24742	3.70	8.03E-04	<i>TMTC4</i>	ILMN_1347	1.59	3.27E-03	<i>FLCN</i>	ILMN_27063	-1.76	4.12E-03	<i>ZBTB32</i>	ILMN_2617	-3.17	8.68E-04
<i>SLC4A11</i>	ILMN_14571	3.65	7.40E-04	<i>ADA</i>	ILMN_8067	1.57	1.42E-02	<i>TBC1D3C</i>	ILMN_137028	-1.76	5.38E-03	<i>PKHD1L1</i>	ILMN_18858	-3.21	1.23E-02
<i>ACOXL</i>	ILMN_6767	3.60	2.47E-03	<i>C7ORF49</i>	ILMN_9001	1.56	4.09E-03	<i>PPP1R15A</i>	ILMN_1024	-1.77	1.32E-03	<i>LCE1D</i>	ILMN_24033	-3.34	5.64E-04
<i>RORA</i>	ILMN_114182	3.55	2.02E-02	<i>PACS2</i>	ILMN_22761	1.55	5.70E-03	<i>RPL39L</i>	ILMN_26587	-1.77	2.81E-02	<i>CD27</i>	ILMN_4066	-3.36	5.53E-04
<i>SELIL3</i>	ILMN_5957	3.37	3.56E-03	<i>RSU1</i>	ILMN_20461	1.55	1.34E-05	<i>PDP2</i>	ILMN_9168	-1.77	8.55E-04	<i>GPT2</i>	ILMN_5354	-3.37	1.09E-03
<i>HNRPLL</i>	ILMN_4564	3.33	1.20E-02	<i>MFSD6L</i>	ILMN_18512	1.53	8.32E-03	<i>CDK2AP2</i>	ILMN_7457	-1.79	1.56E-02	<i>PRSS16</i>	ILMN_10360	-3.38	1.27E-02
<i>LBH</i>	ILMN_34703	3.31	5.39E-04	<i>CERK</i>	ILMN_24122	1.52	4.02E-03	<i>PKMYT1</i>	ILMN_1154	-1.82	1.15E-03	<i>CYP11A1</i>	ILMN_27808	-3.46	3.54E-04
<i>REL</i>	ILMN_10908	3.09	5.55E-03	<i>SLC5A6</i>	ILMN_880	1.52	4.90E-03	<i>HMGCS1</i>	ILMN_18980	-1.83	1.55E-03	<i>CTH</i>	ILMN_4045	-3.47	2.66E-03
<i>NFKBIZ</i>	ILMN_16362	3.08	4.94E-04	<i>MGC16169</i>	ILMN_16160	1.52	2.06E-03	<i>CST3</i>	ILMN_15664	-1.86	1.02E-02	<i>MSX1</i>	ILMN_137891	-3.67	3.67E-03
<i>GSN</i>	ILMN_137841	2.87	1.32E-02	<i>PPAPDC2</i>	ILMN_4922	1.51	8.37E-03	<i>ENO2</i>	ILMN_15419	-1.87	2.21E-03	<i>LCE1E</i>	ILMN_138807	-3.69	5.00E-03
<i>NMT2</i>	ILMN_7780	2.73	2.01E-02	Downregulated protein-encoding genes				<i>RNPC2</i>	ILMN_20445	-1.89	1.52E-03	<i>CXORF57</i>	ILMN_27534	-3.71	8.07E-03
<i>PTK2/FAK</i>	ILMN_20899	2.70	1.18E-03					<i>HPCAL1</i>	ILMN_11657	-1.89	2.10E-03	<i>ITIH1</i>	ILMN_25855	-3.83	1.39E-02
<i>ITPR2</i>	ILMN_13530	2.64	1.15E-02	<i>SLC20A1</i>	ILMN_7081	-1.51	8.07E-04	<i>SLC7A1</i>	ILMN_22619	-1.92	1.90E-03	<i>SIT1</i>	ILMN_18699	-3.89	1.89E-04
<i>TNFSF4/CD134L</i>	ILMN_8432	2.63	4.93E-03	<i>CDCA7L</i>	ILMN_14646	-1.51	3.57E-03	<i>NUDT8</i>	ILMN_14871	-1.92	9.72E-05	<i>TBC1D8</i>	ILMN_13299	-3.99	3.23E-04
<i>STK17B/DRAK2</i>	ILMN_24781	2.61	3.00E-02	<i>CCDC104</i>	ILMN_2409	-1.52	2.24E-03	<i>ZNF292</i>	ILMN_38501	-1.93	3.85E-03	<i>CKAP4</i>	ILMN_4432	-4.19	3.38E-03
<i>C20ORF108</i>	ILMN_25852	2.60	5.45E-03	<i>SPATA7</i>	ILMN_2515	-1.52	1.91E-03	<i>BCKDHA</i>	ILMN_13270	-1.94	3.94E-06	<i>KCTD12</i>	ILMN_18501	-4.68	8.25E-04
<i>ALDH2</i>	ILMN_17598	2.59	6.53E-03	<i>PGRMC1</i>	ILMN_8714	-1.52	4.07E-03	<i>AFMID</i>	ILMN_5520	-1.95	1.90E-03	<i>SP110</i>	ILMN_2801	-4.75	1.95E-05
<i>RUNX1</i>	ILMN_19125	2.58	6.76E-03	<i>PCK2</i>	ILMN_18787	-1.53	2.13E-03	<i>RHOV</i>	ILMN_27155	-1.96	2.24E-02	<i>HLA-C</i>	ILMN_23822	-5.45	2.26E-03
<i>FAM105A</i>	ILMN_10775	2.58	7.48E-05	<i>ANXA5</i>	ILMN_26606	-1.53	4.32E-03	<i>SLC7A5</i>	ILMN_25446	-1.96	1.93E-02	<i>IL12A</i>	ILMN_28240	-5.71	2.30E-03
<i>CSPG4</i>	ILMN_1596	2.57	2.27E-02	<i>HSP90B1</i>	ILMN_27563	-1.53	1.67E-03	<i>SERPINE2</i>	ILMN_1946	-1.98	1.52E-02	<i>PBX4</i>	ILMN_11004	-5.75	5.55E-03
<i>CD83</i>	ILMN_16705	2.56	2.56E-02	<i>TMEM48</i>	ILMN_26078	-1.53	3.79E-03	<i>ARHGEF17</i>	ILMN_11064	-1.98	3.57E-03	<i>AIM2</i>	ILMN_10231	-5.82	2.59E-03
<i>MIB1</i>	ILMN_5164	2.37	7.78E-03	<i>SNHG4</i>	ILMN_15287	-1.53	9.56E-03	<i>HOXB7</i>	ILMN_137246	-1.98	4.25E-03	<i>INHBE</i>	ILMN_7067	-5.87	5.31E-04
<i>ELL2</i>	ILMN_15317	2.33	3.00E-02	<i>EPS15L1</i>	ILMN_20498	-1.54	5.93E-03	<i>TNFRSF13C/BAFFR</i>	ILMN_22155	-2.00	1.08E-02	<i>COL5A1</i>	ILMN_139036	-6.20	7.99E-03
<i>ALDH4A1</i>	ILMN_10603	2.28	3.10E-03	<i>BNIP1</i>	ILMN_6602	-1.55	6.29E-03	<i>LY9/SLAMF3</i>	ILMN_24363	-2.01	1.94E-03	<i>SCNN1B</i>	ILMN_28619	-6.96	8.95E-03
<i>MUM1</i>	ILMN_23934	2.28	1.89E-02	<i>HPS1</i>	ILMN_2724	-1.55	4.49E-03	<i>POU5F1</i>	ILMN_26895	-2.03	4.69E-04	<i>LCE1B</i>	ILMN_23910	-7.03	1.21E-02
<i>SDCCAG8</i>	ILMN_24496	2.27	8.39E-03	<i>SCD</i>	ILMN_25431	-1.56	8.33E-03	<i>FLT4</i>	ILMN_28031	-2.05	2.23E-03	<i>PHGDH</i>	ILMN_5800	-8.01	2.00E-06

(Continued)

TABLE E1. (Continued)

Gene symbol	Illumina ID	Fold change	t Test	Gene symbol	Illumina ID	Fold change	t Test	Gene symbol	Illumina ID	Fold change	t Test	Gene symbol	Illumina ID	Fold change	t Test
<i>OSBPL3</i>	ILMN_17721	2.16	5.12E-03	<i>AVPI1</i>	ILMN_9920	-1.57	6.29E-03	<i>SHMT2</i>	ILMN_19915	-2.05	1.35E-03	<i>CYP4F3</i>	ILMN_20221	-8.18	6.76E-03
<i>MLLT11</i>	ILMN_21397	2.10	7.95E-03	<i>PPP2R3B</i>	ILMN_5735	-1.57	2.48E-03	<i>ASAH1</i>	ILMN_26236	-2.08	2.49E-04	<i>KCNMB2</i>	ILMN_16032	-8.39	2.31E-03
<i>FAM89B</i>	ILMN_9389	2.09	3.08E-02	<i>ANKRD13A</i>	ILMN_14148	-1.57	3.31E-03	<i>SELM</i>	ILMN_1005	-2.11	1.39E-03	<i>CXCL16</i>	ILMN_29805	-8.63	5.94E-03
<i>C4ORF32</i>	ILMN_18245	2.09	4.18E-03	<i>PLP2</i>	ILMN_21868	-1.61	9.75E-03	<i>FKBP11</i>	ILMN_14765	-2.14	8.55E-03	<i>PRODH</i>	ILMN_17486	-9.20	4.67E-03
<i>CIITA</i>	ILMN_22738	2.08	2.34E-03	<i>GSTM4</i>	ILMN_3050	-1.61	8.10E-03	<i>APOBEC3B</i>	ILMN_5305	-2.17	6.00E-04	<i>UNQ2541</i>	ILMN_16426	-9.49	5.48E-04
<i>RNF170</i>	ILMN_24753	2.06	4.31E-03	<i>SC65</i>	ILMN_21605	-1.61	2.99E-03	<i>SLC3A2</i>	ILMN_12826	-2.17	5.03E-03	<i>LYPD6B</i>	ILMN_5409	-10.07	2.74E-03
<i>F11R</i>	ILMN_29770	2.05	1.48E-02	<i>FLJ21839</i>	ILMN_137244	-1.62	7.42E-04	<i>SLC1A5</i>	ILMN_29291	-2.17	3.05E-04	<i>EMR1</i>	ILMN_12984	-10.72	1.59E-03
<i>JARID1B</i>	ILMN_14812	2.01	3.19E-03	<i>UAP1L1</i>	ILMN_20654	-1.63	1.21E-02	<i>TRIB3</i>	ILMN_21257	-2.18	2.75E-03	<i>NDUFA4L2</i>	ILMN_11091	-14.01	9.29E-03
<i>CXXC4</i>	ILMN_11813	1.99	1.87E-04	<i>PGM3</i>	ILMN_14773	-1.63	3.76E-02	<i>ANG</i>	ILMN_13716	-2.19	1.21E-03	<i>TIAM2</i>	ILMN_9891	-18.63	3.06E-03
<i>KMO</i>	ILMN_10994	1.92	2.75E-03	<i>LILRA6</i>	ILMN_27203	-1.63	4.77E-04	<i>EIF4EBP1</i>	ILMN_6626	-2.21	2.00E-03				
<i>SFMBT2</i>	ILMN_5290	1.90	4.85E-03	<i>XPOT</i>	ILMN_22427	-1.63	5.84E-03	<i>C6ORF223</i>	ILMN_9341	-2.22	7.40E-03				